Applied Mathematical Modelling 34 (2010) 3478–3492

Contents lists available at ScienceDirect

Applied Mathematical Modelling

journal homepage: www.elsevier.com/locate/apm

On the stress singularities and boundary layer in moderately thick functionally graded sectorial plates

A.R. Saidi [a,*], F. Hejripour [a], E. Jomehzadeh [b]

[a] Department of Mechanical Engineering, Shahid Bahonar University of Kerman, Kerman, Iran
[b] Young Researchers Society, Shahid Bahonar University of Kerman, Kerman, Iran

ARTICLE INFO

Article history:
Received 13 October 2009
Received in revised form 17 January 2010
Accepted 12 February 2010
Available online 1 March 2010

Keywords:
Stress singularity
Boundary layer
Functionally graded
Sector plate

ABSTRACT

In this paper, the stress analysis of moderately thick functionally graded sector plate is developed for studying the singularities in vicinity of the vertex and effects of boundary layer. Based on the first-order shear deformation plate theory, the governing partial differential equations are obtained. Using an analytical method, the stretching and bending equilibrium equations are decoupled. Also, introducing a function, called boundary layer function, the three bending equations are converted into two decoupled equations. These equations are solved analytically and the effects of boundary layer function on stress components are shown. Also, the singularities of shear force, moment resultants and boundary layer function are discussed for both salient ($\alpha \leqslant 180$) and re-entrant ($\alpha > 180$) sectorial plates. In order to verify the accuracy of the results, the governing equations are also solved using differential quadrature method (DQM). By comparing the results of exact method with DQM, a good agreement can be seen.

1. Introduction

The sector plates are widely used in engineering problems. The analysis of the sector plates, because of existence a sharp corner on the vertex of sector plate, is encountered some singularities in the moment and shear force resultants. According to the classical thin plate theory, William [1,2] studied corner stress singularities resulting from various boundary conditions in isotropic plates under bending and extension. Dempsey and Sinclair [3] re-examined the stress singularities in isotropic plates under extension by introducing an Airy stress function. Ojikutu et al. [4] used a finite difference scheme to study the stress singularities in laminated composite plates with simply supported radial edges. Leissa et al. [5,6] used the Ritz method and introduced the so-called corner functions as the admissible functions to study the singular behavior for free vibration of thin sectorial plates with re-entrant corners or V-notches. Huang et al. [7] found the closed form solution for the vibration of a sector plate with simply supported radial edges to study the corner stress singularities. They used the first-order shear deformation plate theory to study thick plates by considering a shear correction factor. Burton and Sinclair [8] introduced a stress potential by investigating Williams-type corner stress singularities for isotropic thick plates due to six different combinations of homogeneous boundary conditions around a corner, but the singularities of the shear forces were not represented in their solution. Huang et al. [9] studied the corner stress singularities by using a closed-form solution for the vibration of a Mindlin sector plate with simply supported radial edges. Huang [10] investigated corner stress singularities and obtained the orders of moment and shear force singularities. Kotousov and Lew [11] studied the corner stress singularities for a sector plate within the first-order plate theory by using stress resultant and displacement functions and adapting

* Corresponding author. Tel.: +98 341 2111763; fax: +98 341 2120964.
E-mail address: saidi@mail.uk.ac.ir (A.R. Saidi).

0307-904X/$ - see front matter © 2010 Elsevier Inc. All rights reserved.
doi:10.1016/j.apm.2010.02.036

the eigenfunction expansion approach of Williams. The stress singularities are investigated based on the three-dimensional elasticity theories in many papers. Hartranft [12] used eigenfunction expansion to study three-dimensional crack problems. Xie and Chaudhuri [13] investigated the stress singularity at a biomaterial interface crack front by using three-dimensional elasticity theories. Huang [14] obtained the orders of Williams-type stress singularities under various boundary conditions around a corner by using Lo's high-order plate theory.

The mentioned papers investigate the stress singularities in isotropic, non-isotropic and bi-material plates. The functionally graded materials (FGMs) are composite materials that are used in aerospace, nuclear and other engineering applications. In these materials, the mechanical properties vary along one or more directions, usually along the thickness direction, continuously. Due to this wide applicability, the bending analysis of the FGM plates can be important. Zenkour [15] investigated the bending analysis of FGM plates based on generalized shear deformation theory. Huang and Chang [16] studied the stress singularities for an FGM plate by using the classical thin plate theory.

The usual changes of different parameters in the vicinity of the edges of plates are known as boundary layer phenomenon. The cause of this effect is the existence of the boundary layer function. This function has a significant value in the near of the edges and it is zero in interior zone. The boundary layer was first introduced by Reissner [17,18]. Nossier and Reddy [19] investigated the boundary layer and the transverse displacement in the bending of symmetric laminated plates made of transversely isotropic layer by uncoupling the bending equations into two equations. Nosier et al. [20] used the boundary layer to study two opposite simply supported edges in Mindlin rectangular plates under bending. Jomehzadeh and Saidi [21] investigated the free vibration of transversely isotropic sector plates by using the boundary layer function. Jomehzadeh et al. [22] used an exact analytical solution for bending analysis of functionally graded annular sector plates and investigated the effects of power of FGM, the geometrical characteristics and boundary conditions on the deflection and stresses of the FG sector plates. Recently, Atashipour et al. [23] studied the boundary layer phenomenon in third-order shear deformation theory for bending of isotropic annular sector plates.

In this paper, the five highly coupled partial differential equations of FG sector plate under static loading are decoupled using the boundary layer function. Also, analytical solutions are obtained for stress analysis of FG sector plates with various boundary conditions. The boundary layer function and its effect on the stresses of the FG plate are studied numerically. The effects of plate thickness, boundary conditions and power of functionally graded material are investigated. Since the effect of boundary layer function for FG plates is similar to isotropic and composite plates, this function seems to be material independent. Also, the singularities of the force and moment resultants in vicinity of vertex are discussed in details.

2. Governing equations

Based on the first-order shear deformation plate theory, the displacement field of a sector plate is expressed as:

$$U(r,\theta,z) = u(r,\theta) + z\psi_r(r,\theta), \tag{1a}$$
$$V(r,\theta,z) = v(r,\theta) + z\psi_\theta(r,\theta), \tag{1b}$$
$$W(r,\theta,z) = w(r,\theta), \tag{1c}$$

where u, v and w are the displacement components of the mid-plane in r, θ and z directions, respectively. ψ_r and ψ_θ denote the rotation functions of the transverse normal about θ- and r-axis, respectively.

Using the principle of stationary total potential energy, the governing equations as well as the related boundary conditions along the edges of a functionally graded sector plate can be obtained. The governing equations are [22]

$$A_{11}\left(\frac{\partial^2 u}{\partial r^2}+\frac{1}{r}\frac{\partial u}{\partial r}-\frac{u}{r^2}-\frac{1}{r^2}\frac{\partial v}{\partial \theta}+\frac{1}{r}\frac{\partial^2 v}{\partial r\partial\theta}\right)+A_{33}\left(\frac{1}{r^2}\frac{\partial^2 u}{\partial\theta^2}-\frac{1}{r}\frac{\partial^2 v}{\partial r\partial\theta}-\frac{1}{r^2}\frac{\partial v}{\partial\theta}\right)$$
$$+B_{11}\left(\frac{\partial^2\psi_r}{\partial r^2}+\frac{1}{r}\frac{\partial\psi_r}{\partial r}-\frac{\psi_r}{r^2}-\frac{1}{r^2}\frac{\partial\psi_\theta}{\partial\theta}+\frac{1}{r}\frac{\partial^2\psi_\theta}{\partial r\partial\theta}\right)+B_{33}\left(\frac{1}{r^2}\frac{\partial^2\psi_r}{\partial\theta^2}-\frac{1}{r}\frac{\partial^2\psi_\theta}{\partial r\partial\theta}-\frac{1}{r^2}\frac{\partial\psi_\theta}{\partial\theta}\right)=0, \tag{2a}$$

$$A_{11}\left(\frac{1}{r}\frac{\partial^2 u}{\partial r\partial\theta}+\frac{1}{r^2}\frac{\partial u}{\partial\theta}+\frac{1}{r^2}\frac{\partial^2 v}{\partial\theta^2}\right)+A_{33}\left(\frac{1}{r^2}\frac{\partial u}{\partial\theta}-\frac{1}{r}\frac{\partial^2 u}{\partial r\partial\theta}+\frac{\partial^2 v}{\partial r^2}+\frac{1}{r}\frac{\partial v}{\partial r}-\frac{v}{r^2}\right)+B_{11}\left(\frac{1}{r}\frac{\partial^2\psi_r}{\partial r\partial\theta}+\frac{1}{r^2}\frac{\partial\psi_r}{\partial\theta}+\frac{1}{r^2}\frac{\partial^2\psi_\theta}{\partial\theta^2}\right)$$
$$+B_{33}\left(\frac{1}{r^2}\frac{\partial\psi_r}{\partial\theta}-\frac{1}{r}\frac{\partial^2\psi_r}{\partial r\partial\theta}+\frac{\partial^2\psi_\theta}{\partial r^2}+\frac{1}{r}\frac{\partial\psi_\theta}{\partial r}-\frac{\psi_\theta}{r^2}\right)=0, \tag{2b}$$

$$B_{11}\left(\frac{\partial^2 u}{\partial r^2}+\frac{1}{r}\frac{\partial u}{\partial r}-\frac{u}{r^2}-\frac{1}{r^2}\frac{\partial v}{\partial\theta}+\frac{1}{r}\frac{\partial^2 v}{\partial r\partial\theta}\right)+B_{33}\left(\frac{1}{r^2}\frac{\partial^2 u}{\partial\theta^2}-\frac{1}{r}\frac{\partial^2 v}{\partial r\partial\theta}-\frac{1}{r^2}\frac{\partial v}{\partial\theta}\right)$$
$$+D_{11}\left(\frac{\partial^2\psi_r}{\partial r^2}+\frac{1}{r}\frac{\partial\psi_r}{\partial r}-\frac{\psi_r}{r^2}-\frac{1}{r^2}\frac{\partial\psi_\theta}{\partial\theta}+\frac{1}{r}\frac{\partial^2\psi_\theta}{\partial r\partial\theta}\right)+D_{33}\left(\frac{1}{r^2}\frac{\partial^2\psi_r}{\partial\theta^2}-\frac{1}{r}\frac{\partial^2\psi_\theta}{\partial r\partial\theta}-\frac{1}{r^2}\frac{\partial\psi_\theta}{\partial\theta}\right)-K^2A_{33}\left(\psi_r+\frac{\partial w}{\partial r}\right)=0, \tag{2c}$$

$$B_{11}\left(\frac{1}{r}\frac{\partial^2 u}{\partial r\partial\theta}+\frac{1}{r^2}\frac{\partial u}{\partial\theta}+\frac{1}{r^2}\frac{\partial^2 v}{\partial\theta^2}\right)+B_{33}\left(\frac{1}{r^2}\frac{\partial u}{\partial\theta}-\frac{1}{r}\frac{\partial^2 u}{\partial r\partial\theta}+\frac{\partial^2 v}{\partial r^2}+\frac{1}{r}\frac{\partial v}{\partial r}-\frac{v}{r^2}\right)+D_{11}\left(\frac{1}{r}\frac{\partial^2\psi_r}{\partial r\partial\theta}+\frac{1}{r^2}\frac{\partial\psi_r}{\partial\theta}+\frac{1}{r^2}\frac{\partial^2\psi_\theta}{\partial\theta^2}\right)$$
$$+D_{33}\left(\frac{1}{r^2}\frac{\partial\psi_r}{\partial\theta}-\frac{1}{r}\frac{\partial^2\psi_r}{\partial r\partial\theta}+\frac{\partial^2\psi_\theta}{\partial r^2}+\frac{1}{r}\frac{\partial\psi_\theta}{\partial r}-\frac{\psi_\theta}{r^2}\right)-K^2A_{33}\left(\psi_\theta+\frac{1}{r}\frac{\partial w}{\partial\theta}\right)=0, \tag{2d}$$

$$K^2A_{33}\left(\frac{\partial^2 w}{\partial r^2}+\frac{1}{r}\frac{\partial w}{\partial r}+\frac{1}{r^2}\frac{\partial^2 w}{\partial\theta^2}+\frac{\partial\psi_r}{\partial r}+\frac{\psi_r}{r}+\frac{1}{r}\frac{\partial\psi_\theta}{\partial\theta}\right)+p_z=0 \tag{2e}$$

and the boundary conditions are defined as

$$\begin{aligned}
&\delta u=0: N_r n_r+N_{r\theta}n_\theta=0,\\
&\delta v=0: N_{r\theta}n_r+N_\theta n_\theta=0,\\
&\delta\psi_r=0: M_r n_r+M_{r\theta}n_\theta=0,\\
&\delta\psi_\theta=0: M_{r\theta}n_r+M_\theta n_\theta=0,\\
&\delta w=0: Q_r n_r+Q_\theta n_\theta=0,
\end{aligned} \tag{3}$$

where K^2 is the shear correction factor which in the present study is assumed to be 5/6.

Also the integration coefficients are defined as

$$A_{11}=\frac{1}{1-\nu^2}\int_{-h/2}^{h/2}E(z,T)dz,\quad A_{33}=\frac{1}{2(1+\nu)}\int_{-h/2}^{h/2}E(z,T)dz, \tag{4a}$$
$$B_{11}=\frac{1}{1-\nu^2}\int_{-h/2}^{h/2}zE(z,T)dz,\quad B_{33}=\frac{1}{2(1+\nu)}\int_{-h/2}^{h/2}zE(z,T)dz, \tag{4b}$$
$$D_{11}=\frac{1}{1-\nu^2}\int_{-h/2}^{h/2}z^2E(z,T)dz,\quad D_{33}=\frac{1}{2(1+\nu)}\int_{-h/2}^{h/2}z^2E(z,T)dz, \tag{4c}$$

where $E(z,T)$ is the Young modulus of the FG sector plate which is assumed to be temperature dependent and to vary along the thickness direction based on a power law function as

$$E(z,T)=E_c+(E_c-E_m)(z/h-1/2)^n, \tag{5}$$

where subscripts c and m are related to ceramic and metal, respectively. Also, n is the power of functionally graded material. The Young modulus of the ceramic and metal can be defined as a function of the temperature as follows [24]:

$$E=E_0(E_{-1}T^{-1}+1+E_1T+E_2T^2+E_3T^3), \tag{6}$$

where $E_0,\ E_{-1},\ E_1,\ E_2$ and E_3 are the temperature coefficients which are given in Table 1.

$M_r,\ M_\theta$ and $M_{r\theta}$ are the moment resultants which are defined as

$$M_r=\int_{-h/2}^{h/2}z\sigma_r\,dz, \tag{7a}$$
$$M_\theta=\int_{-h/2}^{h/2}z\sigma_\theta\,dz, \tag{7b}$$
$$M_{r\theta}=\int_{-h/2}^{h/2}z\sigma_{r\theta}\,dz, \tag{7c}$$

Table 1
The temperature coefficients of the ceramic and metal young modulus ($E*10^9$), Ref [25].

Material	E_0	E_{-1}	E_1	E_2	E_3
SUS304	201.04	0	3.079e−4	−6.534e−7	0
Si3N4	348.43	0	−3.070e−4	2.160e−7	−8.946e−11
Ti–6Al–4V	122.56	0	−4.586e−4	0	0
Aluminum oxide	349.55	0	−3.853e−4	4.027e−7	−1.673e−10

Also N_r, N_θ and $N_{r\theta}$ are the in-plane force resultants as

$$N_r = \int_{-h/2}^{h/2} \sigma_r \, dz, \tag{8a}$$

$$N_\theta = \int_{-h/2}^{h/2} \sigma_\theta \, dz, \tag{8b}$$

$$N_{r\theta} = \int_{-h/2}^{h/2} \sigma_{r\theta} \, dz, \tag{8c}$$

And the shear force resultants Q_r and Q_θ are as follows:

$$Q_r = K^2 \int_{-h/2}^{h/2} \sigma_{rz} \, dz, \tag{9a}$$

$$Q_\theta = K^2 \int_{-h/2}^{h/2} \sigma_{r\theta} \, dz, \tag{9b}$$

where σ_r, σ_θ, $\sigma_{r\theta}$ and σ_{rz} are stress components.

The five highly coupled partial differential equations (2) can be rewritten as

$$A_{11}\frac{\partial \varphi_1}{\partial r} + A_{33}\frac{1}{r}\frac{\partial \varphi_2}{\partial \theta} + B_{11}\frac{\partial \varphi_3}{\partial r} + B_{33}\frac{1}{r}\frac{\partial \varphi_4}{\partial \theta} = 0, \tag{10a}$$

$$A_{11}\frac{1}{r}\frac{\partial \varphi_1}{\partial \theta} - A_{33}\frac{\partial \varphi_2}{\partial r} + B_{11}\frac{1}{r}\frac{\partial \varphi_3}{\partial \theta} - B_{33}\frac{\partial \varphi_4}{\partial r} = 0, \tag{10b}$$

$$B_{11}\frac{\partial \varphi_1}{\partial r} + B_{33}\frac{1}{r}\frac{\partial \varphi_2}{\partial \theta} + D_{11}\frac{\partial \varphi_3}{\partial r} + D_{33}\frac{1}{r}\frac{\partial \varphi_4}{\partial \theta} - K^2 A_{33}\left(\psi_r + \frac{\partial w}{\partial r}\right) = 0, \tag{10c}$$

$$B_{11}\frac{1}{r}\frac{\partial \varphi_1}{\partial \theta} - B_{33}\frac{\partial \varphi_2}{\partial r} + D_{11}\frac{1}{r}\frac{\partial \varphi_3}{\partial \theta} - D_{33}\frac{\partial \varphi_4}{\partial r} - K^2 A_{33}\left(\psi_\theta + \frac{1}{r}\frac{\partial w}{\partial \theta}\right) = 0, \tag{10d}$$

$$K^2 A_{33}(\nabla^2 w + \varphi_3) + p_z = 0, \tag{10e}$$

where $\nabla^2 \left(\nabla^2 = \partial^2/\partial r^2 + \frac{1}{r}\partial/\partial r + \frac{1}{r^2}\partial^2/\partial\theta^2\right)$ is the two-dimensional Laplace operator in polar coordinate. Also, the functions φ_1, φ_2, φ_3, and φ_4 are defined as

$$\begin{aligned} \varphi_1 &= \frac{\partial u}{\partial r} + \frac{u}{r} + \frac{1}{r}\frac{\partial v}{\partial \theta}, \quad \varphi_2 = \frac{1}{r}\frac{\partial u}{\partial \theta} - \frac{\partial v}{\partial r} - \frac{v}{r}, \\ \varphi_3 &= \frac{\partial \psi_r}{\partial r} + \frac{\psi_r}{r} + \frac{1}{r}\frac{\partial \psi_\theta}{\partial \theta}, \quad \varphi_4 = \frac{1}{r}\frac{\partial \psi_r}{\partial \theta} - \frac{\partial \psi_\theta}{\partial r} - \frac{\psi_\theta}{r}. \end{aligned} \tag{11}$$

Applying some algebraic operations, the governing equations (10) can be converted into four equations as

$$\widehat{D}\nabla^4 w = p_z - \frac{\widehat{D}}{K^2 A_{11}}\nabla^2 p_z, \tag{12a}$$

$$\widehat{C}\nabla^2 \varphi_4 - K^2 \widehat{A}\varphi_4 = 0, \tag{12b}$$

$$\nabla^2 \varphi_2 = -\frac{B_{11}}{A_{11}}\nabla^2 \varphi_4, \tag{12c}$$

$$\nabla^2 \varphi_1 = -\frac{B_{11}}{A_{11}}\nabla^2 \varphi_3, \tag{12d}$$

where $\widehat{D} = D_{11} - B_{11}^2/A_{11}$ is the flexural rigidity of the FG plate. Also, $\widehat{A}$ and $\widehat{C}$ are A_{33} and $D_{33} - B_{11}B_{33}/A_{11}$, respectively.

The rotation functions ψ_r and ψ_θ can be derived easily as follows:

$$\psi_r = -\frac{\partial}{\partial r}\left(w + \frac{\widehat{D}}{K^2\widehat{A}}\nabla^2 w + \frac{\widehat{D}}{K^4\widehat{A}^2}p_z\right) + \frac{\widehat{C}}{K^2\widehat{A}}\frac{1}{r}\varphi_{4,\theta}, \tag{13a}$$

$$\psi_\theta = -\frac{1}{r}\frac{\partial}{\partial \theta}\left(w + \frac{\widehat{D}}{K^2\widehat{D}}\nabla^2 w + \frac{\widehat{D}}{K^4\widehat{A}^2}p_z\right) - \frac{\widehat{C}}{K^2\widehat{A}}\varphi_{4,r}. \tag{13b}$$

Also, the force and moment resultants can be obtained in terms of transverse deflection w and the function φ_4. It will be shown that the function φ_4 has a boundary layer behavior. Thus, like the homogeneous plates [19], this function will be known as the boundary layer function.

3. Solution

It is assumed that the FG sector plate with radius a and sector angle α is simply supported along two radial edges and carrying out the uniform distributed load P_0 (Fig. 1). The transverse displacement, the boundary layer function φ_4 and the transverse load can be expanded in their series solution as

$$w=\sum_{m=1,3,\ldots}^{\infty} w_m(r)\sin(\beta_m\theta),\quad \varphi_4=\sum_{m=1,3,\ldots}^{\infty}\varphi_m(r)\cos(\beta_m\theta),\quad p_z=\sum_{m=1,3,\ldots}^{\infty} p_m\sin(\beta_m\theta), \tag{14}$$

where β_m is $m\pi/\alpha$ and p_m is defined as

$$p_m=\frac{2}{\alpha}\int_0^{\alpha} P_0\sin(\beta_m\theta)d\theta. \tag{15}$$

Substituting Eq. (14) into the two decoupled equations (12a) and (12b) and solving the resulting ordinary differential equations, the transverse displacement for $\beta_m\neq 2,4$ and the function φ_m are obtained as

$$w_m(r)=C_{1m}r^{\beta_m}+C_{2m}r^{-\beta_m}+C_{3m}r^{2-\beta_m}+C_{4m}r^{2+\beta_m}+\frac{p_m r^2(K^2\widehat{A}r^2+\widehat{D}\beta_m^2-16\widehat{D})}{K^2\widehat{A}\,\widehat{D}(\beta_m^2-16)(\beta_m^2-4)}, \tag{16a}$$

$$\varphi_m(r)=C_{5m}I_{\beta_m}(\mu r)+C_{6m}K_{\beta_m}(\mu r), \tag{16b}$$

where I_{β_m} and K_{β_m} are the modified Bessel functions of the first and second kinds, respectively. Also μ is $\sqrt{K^2\widehat{A}/\widehat{C}}$. For $\beta_m=2$ and 4, the solution of boundary layer functions is the same as Eq. (16b) and the transverse displacement is obtained as

$$w_m=\begin{cases}\left(p_m\left(-\frac{11r^4}{576\widehat{D}}-\frac{1}{4}\frac{r^2\ln(r)}{K^2\widehat{A}}+\frac{r^2}{16K^2\widehat{A}}+\frac{1}{48}\frac{r^4\ln(r)}{\widehat{D}}\right)+C_1\frac{r^2}{2}-C_2\frac{1}{2r^2}+C_3+C_4\frac{r^4}{4}\right)\sin(2\theta) & \text{for } \beta_m=2,\\ \left(-\frac{p_m r^2}{2304}\left(\frac{5K^2\widehat{A}r^2-192\widehat{D}+24\ln(r)K^2\widehat{A}r^2}{\widehat{D}K^2\widehat{A}}\right)+C_1r^4+C_2\frac{1}{r^4}+C_3\frac{1}{r^2}+C_4r^6\right)\sin(4\theta) & \text{for } \beta_m=4.\end{cases} \tag{17}$$

It can be seen that Eqs. (12c) and (12d) are exactly satisfied by assuming the in-plane displacements as

$$u=-\frac{B_{11}}{A_{11}}\psi_r, \tag{18a}$$

$$v=-\frac{B_{11}}{A_{11}}\psi_\theta. \tag{18b}$$

These relations are valid for some types of boundary conditions as can be seen afterward. Also, substituting Eqs. (16) into Eqs. (13) the rotation functions can be obtained as

$$\psi_r=\left(-C_{1m}\beta_m r^{\beta_m-1}+C_{2m}\beta_m r^{-\beta_m-1}-C_{3m}\frac{4\widehat{D}\beta_m(\beta_m-1)r^{-\beta_m-1}-K^2\widehat{A}(\beta_m-2)r^{-\beta_m+1}}{K^2\widehat{A}}\right.$$
$$\left.-C_{4m}\frac{4\widehat{D}\beta_m(\beta_m+1)r^{\beta_m-1}+K^2\widehat{A}(\beta_m+2)r^{\beta_m+1}}{K^2\widehat{A}}-C_{5m}\frac{\widehat{C}\beta_m I_{\beta_m}(\mu r)}{K^2\widehat{A}r}-C_{6m}\frac{\widehat{C}\beta_m K_{\beta_m}(\mu r)}{K^2\widehat{A}r}-\frac{4p_m r^3}{\widehat{D}(\beta_m^2-16)(\beta_m^2-4)}\right)\sin(\beta_m\theta), \tag{19a}$$

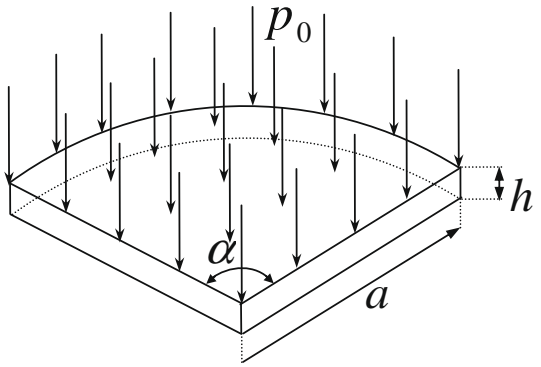

Fig. 1. The geometry of the sector plate.

$$\psi_\theta = \left(-C_{1m}\beta_m r^{\beta_m-1} - C_{2m}\beta_m r^{-\beta_m-1} + C_{3m}\frac{4\widehat{D}\,\beta_m(\beta_m-1)r^{-\beta_m-1} - K^2\widehat{A}\,\beta_m r^{-\beta_m+1}}{K^2\widehat{A}} \right.$$
$$- C_{4m}\frac{4\widehat{D}\,\beta_m(\beta_m+1)r^{\beta_m-1} + K^2\widehat{A}\,\beta_m r^{\beta_m+1}}{K^2\widehat{A}} - C_{5m}\widehat{C}\,\frac{\beta_m I_{\beta_m}(\mu r) + r\mu I_{\beta_m+1}(\mu r)}{K^2\widehat{A}\,r}$$
$$\left. + C_{6m}\widehat{C}\,\frac{-\beta_m K_{\beta_m}(\mu r) + r\mu K_{\beta_m+1}(\mu r)}{K^2\widehat{A}\,r} - \frac{p_m\beta_m r^3}{\widehat{D}(\beta_m^2-16)(\beta_m^2-4)} \right)\cos(\beta_m\theta). \tag{19b}$$

To determine the six unknown coefficients ($C_{im},\ i=1,\dots,6$), the regularity conditions at $r=0$ and the boundary conditions at $r=a$ should be applied. Five regularly conditions at $r=0$ can be considered as

$$w = 0, \tag{20a}$$
$$u = finite, \tag{20b}$$
$$v = finite, \tag{20c}$$
$$\psi_r = finite, \tag{20d}$$
$$\psi_\theta = finite. \tag{20e}$$

Based on the relation (18), it can be seen that satisfying the regularity conditions (20d) and (20e) is equivalent to (20b) and (20c). Therefore, it is sufficient to apply only the conditions (20a), (20d) and (20e). In order to satisfy Eq. (20a), it can be concluded that since the value of β_m is larger than zero, the coefficient C_{2m} should be vanished, namely

$$C_{2m} = 0. \tag{21}$$

The modified Bessel function of the first kind can be expanded in term of its power series as follow:

$$I_{\beta_m}(\mu r) = \sum_{k=0}^{\infty}\frac{\left(\frac{\mu r}{2}\right)^{\beta_m+2k}}{k!\Gamma(k+\beta_m+1)}, \tag{22}$$

where Γ is the gamma function. Also, the modified Bessel function of the second kind can be expressed in term of the first kind as

$$K_{\beta_m}(\mu r) = \frac{\pi}{2\sin(\beta_m\pi)}[I_{-\beta_m}(\mu r) - I_{\beta_m}(\mu r)]. \tag{23}$$

Upon substituting Eqs. (22) and (23) into Eqs. (19), the rotation functions ψ_r and ψ_θ are obtained in terms of power series as

$$\psi_r = \left(-C_{1m}\beta_m r^{\beta_m-1} + C_{2m}\beta_m r^{-\beta_m-1} - C_{3m}\frac{4\widehat{D}\,\beta_m(\beta_m-1)r^{-\beta_m-1} - K^2\widehat{A}(\beta_m-2)r^{-\beta_m+1}}{K^2\widehat{A}} \right.$$
$$- C_{4m}\frac{4\widehat{D}\,\beta_m(\beta_m+1)r^{\beta_m-1} + K^2\widehat{A}(\beta_m+2)r^{\beta_m+1}}{K^2\widehat{A}} - C_{5m}\frac{\widehat{C}\,\beta_m\sum_{k=0}^{\infty}\frac{\left(\frac{\mu}{2}\right)^{\beta_m+2k}r^{\beta_m+2k-1}}{k!\Gamma(k+\beta_m+1)}}{K^2\widehat{A}}$$
$$\left. - C_{6m}\frac{\widehat{C}\,\beta_m\pi}{2K^2\widehat{A}\,\sin(\beta_m\pi)}\left(\sum_{k=0}^{\infty}\frac{\left(\frac{\mu}{2}\right)^{-\beta_m+2k}r^{-\beta_m+2k-1}}{k!\Gamma(k-\beta_m+1)} - \sum_{k=0}^{\infty}\frac{\left(\frac{\mu}{2}\right)^{\beta_m+2k}r^{\beta_m+2k-1}}{k!\Gamma(k+\beta_m+1)}\right) - \frac{4p_m r^3}{\widehat{D}(\beta_m^2-16)(\beta_m^2-4)} \right)\sin(\beta_m\theta), \tag{24a}$$

$$\psi_\theta = \left(-C_{1m}\beta_m r^{\beta_m-1} - C_{2m}\beta_m r^{-\beta_m-1} + C_{3m}\frac{4\widehat{D}\,\beta_m(\beta_m-1)r^{-\beta_m-1} - K^2\widehat{A}\,\beta_m r^{-\beta_m+1}}{K^2\widehat{A}} \right.$$
$$- C_{4m}\frac{4\widehat{D}\,\beta_m(\beta_m+1)r^{\beta_m-1} + K^2\widehat{A}\,\beta_m r^{\beta_m+1}}{K^2\widehat{A}} - C_{5m}\frac{\widehat{C}}{K^2\widehat{A}}\left(\beta_m\sum_{k=0}^{\infty}\frac{\left(\frac{\mu}{2}\right)^{\beta_m+2k}r^{\beta_m+2k-1}}{k!\Gamma(k+\beta_m+1)} + \sum_{k=0}^{\infty}\frac{\mu\left(\frac{\mu r}{2}\right)^{\beta_m+2k+1}}{k!\Gamma(k+\beta_m+2)}\right)$$
$$+ C_{6m}\frac{\widehat{C}\,\pi}{2K^2\widehat{A}\,\sin(\beta_m\pi)}\left(-\sum_{k=0}^{\infty}\frac{\beta_m\left(\frac{\mu}{2}\right)^{-\beta_m+2k}r^{-\beta_m+2k-1}}{k!\Gamma(k-\beta_m+1)} + \sum_{k=0}^{\infty}\frac{\beta_m\left(\frac{\mu}{2}\right)^{\beta_m+2k}r^{\beta_m+2k-1}}{k!\Gamma(k+\beta_m+1)}\right.$$
$$\left. \left. + \sum_{k=0}^{\infty}\frac{\mu\left(\frac{\mu r}{2}\right)^{-\beta_m+2k+1}}{k!\Gamma(k-\beta_m+2)} - \sum_{k=0}^{\infty}\frac{\mu\left(\frac{\mu r}{2}\right)^{\beta_m+2k+1}}{k!\Gamma(k+\beta_m+2)}\right) - \frac{p_m\beta_m r^3}{\widehat{D}(\beta_m^2-16)(\beta_m^2-4)}\right)\cos(\beta_m\theta). \tag{24b}$$

In order to satisfy the regularity condition (20d) as r approaches zero, it is convenient to divide the β_m into two intervals $0 < \beta_m < 1$ and $\beta_m \geqslant 1$.

While $0 < \beta_m < 1$, some terms of the limit containing $r^{-\beta_m-1}$ and r^{β_m-1} in Eq. (24a) do not vanish for $k = 0$. To satisfy Eq. (24a), the coefficients of these terms should be equal to zero as follows:

$$C_{2m} - C_{3m}\left(\frac{4\widehat{D}(\beta_m-1)}{K^2\widehat{A}}\right) - C_{6m}\frac{\widehat{C}\,\pi\left(\frac{\mu}{2}\right)^{-\beta_m}}{2K^2\widehat{A}\,\sin(\beta_m\pi)\Gamma(-\beta_m+1)} = 0, \tag{25a}$$

$$-C_{1m} - C_{4m}\left(\frac{4\widehat{D}(\beta_m+1)}{K^2\widehat{A}}\right) - C_{5m}\frac{\widehat{C}\left(\frac{\mu}{2}\right)^{\beta_m}}{K^2\widehat{A}\,\Gamma(\beta_m+1)} + C_{6m}\frac{\widehat{C}\,\pi\left(\frac{\mu}{2}\right)^{\beta_m}}{2K^2\widehat{A}\,\sin(\beta_m\pi)\Gamma(\beta_m+1)} = 0. \tag{25b}$$

Using Eqs. (25) and (21), the coefficients C_{4m} and C_{6m} can be obtained in terms of C_{1m}, C_{3m} and C_{5m} as

$$C_{6m} = -C_{3m}\frac{8\widehat{D}(\beta_m-1)\sin(\beta_m\pi)\Gamma(-\beta_m+1)}{\widehat{C}\,\pi\left(\frac{\mu}{2}\right)^{-\beta_m}}, \tag{26a}$$

$$C_{4m} = -\frac{1}{4}\frac{C_{1m}K^2\widehat{A}\left(\frac{\mu}{2}\right)^{-\beta_m}\Gamma(\beta_m+1) + C_{5m}\widehat{C} + 4C_{3m}\widehat{D}\,\Gamma(-\beta_m+1)\left(\frac{\mu}{2}\right)^{\beta_m}(\beta_m-1)}{\widehat{D}(\beta_m+1)\left(\frac{\mu}{2}\right)^{-\beta_m}\Gamma(\beta_m+1)}. \tag{26b}$$

Also, the coefficients C_{1m}, C_{3m} and C_{5m} are obtained by applying the boundary equations at $r = a$.

When $\beta_m > 1$, the terms contain $r^{-\beta_m-1}$ and $r^{1-\beta_m}$ in Eq. (24a) are infinite. Therefore, their coefficients should be vanished, namely

$$C_{2m} - C_{3m}\left(\frac{4\widehat{D}(\beta_m-1)}{K^2\widehat{A}}\right) - C_{6m}\frac{\widehat{C}\,\pi\left(\frac{\mu}{2}\right)^{-\beta_m}}{2K^2\widehat{A}\,\sin(\beta_m\pi)\Gamma(-\beta_m+1)} = 0, \tag{27a}$$

$$C_{3m}(\beta_m - 2) = 0. \tag{27b}$$

Using Eqs. (21) and (27) the coefficients C_{3m} and C_{6m} are obtained as

$$C_{3m} = C_{6m} = 0. \tag{28}$$

In this case $\beta_m \neq 2, 4$, doing the same procedure as $\beta_m > 1$, It can be seen that $C_2 = C_3 = C_6 = 0$.

To satisfy the last regularity condition (20e), as r approaches zero, it should be considered two intervals $0 < \beta_m < 1$ and $\beta_m \geqslant 1$, again.

In the case $0 < \beta_m < 1$, some terms of the limit in Eq. (24b) do not vanish for $k = 0$ which containing $r^{-\beta_m-1}$ and r^{β_m-1}. To satisfy Eq. (24b), the coefficients of these terms must be vanished, that is

$$C_{2m} - C_{3m}\left(\frac{4\widehat{D}(\beta_m-1)}{K^2\widehat{A}}\right) - C_{6m}\frac{\widehat{C}\,\pi\left(\frac{\mu}{2}\right)^{-\beta_m}}{2K^2\widehat{A}\,\sin(\beta_m\pi)\Gamma(-\beta_m+1)} = 0, \tag{29a}$$

$$-C_{1m} - C_{4m}\left(\frac{4\widehat{D}(\beta_m+1)}{K^2\widehat{A}}\right) - C_{5m}\frac{\widehat{C}\left(\frac{\mu}{2}\right)^{\beta_m}}{K^2\widehat{A}\,\Gamma(\beta_m+1)} + C_{6m}\frac{\widehat{C}\,\pi\left(\frac{\mu}{2}\right)^{\beta_m}}{2K^2\widehat{A}\,\sin(\beta_m\pi)\Gamma(\beta_m+1)} = 0. \tag{29b}$$

In the case $\beta_m \geqslant 1$, the coefficients of $r^{-\beta_m-1}$ and $r^{1-\beta_m}$ should be zero, then

$$C_{2m} - C_{3m}\left(\frac{4\widehat{D}(\beta_m-1)}{K^2\widehat{A}}\right) - C_{6m}\frac{\widehat{C}\,\pi\left(\frac{\mu}{2}\right)^{-\beta_m}}{2K^2\widehat{A}\,\sin(\beta_m\pi)\Gamma(-\beta_m+1)} = 0, \tag{30a}$$

$$C_{3m}\beta_m = 0. \tag{30b}$$

It can be seen that Eqs. (29) and (30) are the same as relations (25) and (27) which have been obtained from applying the second regularity condition (20d).

In order to obtain the unknown coefficients C_{1m}, C_{3m} and C_{5m}, the boundary condition at the circular edge of the FG circular plate should be applied. The circular edge at $r = a$ can be simply supported (type 2), clamped or free with following conditions:

Simply supported (type 2) :

$$v = 0, \quad N_r = 0, \quad w = 0, \quad \psi_\theta = 0, \quad M_r = 0, \tag{31a}$$

Clamped :

$$u = 0, \quad v = 0, \quad w = 0, \quad \psi_r = 0, \quad \psi_\theta = 0, \tag{31b}$$

Free :

$$N_r = 0, \quad N_{r\theta} = 0, \quad Q_r = 0, \quad M_r = 0, \quad M_{r\theta} = 0. \tag{31c}$$

Based on the relations (18), it can be seen that applying two last conditions in each of the boundary conditions (31) will exactly satisfy the two first conditions, i.e. satisfying the two last conditions for simply supported edge ($\psi_\theta = 0,\ M_r = 0$) will spontaneously satisfy two fist conditions ($v = 0,\ N_r = 0$) due to relations (18). Therefor, in order to determine the remaining unknown coefficients of FG plate, it is sufficient to apply the three last conditions of Eq. (31) at $r = a$.

4. Singularities in boundary layer function, moment and shear force resultants

It should be noticed that the modified Bessel functions of second kind is singular at $r = 0$. Therefore, the boundary layer function in Eq. (15b) is singular for $0 < \beta_m < 1$.

Also, to study the singularity in the moment and shear force resultants in all intervals of β_m, the moment and shear force resultants can be obtained by using Eqs. (7) and (9). Expressing the Bessel function in terms of their power series, the moment and shear force resultants are written as

$$M_r = \Big(L_1C_{3m}r^{-\beta_m} + (L_2C_{2m} + L_3C_{3m} + L_4C_{6m})r^{-\beta_m-2} + (L_5C_{1m} + L_6C_{4m} + L_7C_{5m} + L_8C_{6m})r^{\beta_m-2} + L_9C_{4m}r^{\beta_m} + \frac{L_{10}p_mr^2}{(\beta_m^2-4)(\beta_m^2-16)}\Big)\sin(\beta_m\theta), \tag{32a}$$

$$M_\theta = \Big(L_{11}C_{3m}r^{-\beta_m} + (L_{12}C_{2m} + L_{13}C_{3m} + L_{14}C_{6m})r^{-\beta_m-2} + (L_{15}C_{1m} + L_{16}C_{4m} + L_{17}C_{5m} + L_{18}C_{6m})r^{\beta_m-2} + L_{19}C_{4m}r^{\beta_m} + \frac{L_{20}p_mr^2}{(\beta_m^2-4)(\beta_m^2-16)}\Big)\sin(\beta_m\theta), \tag{32b}$$

$$M_{r\theta} = \Big(L_{21}C_{3m}r^{-\beta_m} + (L_{22}C_{2m} + L_{23}C_{3m} + L_{24}C_{6m})r^{-\beta_m-2} + (L_{25}C_{1m} + L_{26}C_{4m} + L_{27}C_{5m} + L_{28}C_{6m})r^{\beta_m-2} + L_{29}C_{4m}r^{\beta_m} + \frac{L_{30}p_mr^2}{(\beta_m^2-4)(\beta_m^2-16)}\Big)\cos(\beta_m\theta), \tag{32c}$$

$$Q_r = \Big((L_{31}C_{3m} + L_{32}C_{6m})r^{-\beta_m-1} + (L_{33}C_{4m} + L_{34}C_{5m} + L_{35}C_{6m})r^{\beta_m-1} + \frac{p_mr}{(\beta_m-4)}\Big)\sin(\beta_m\theta), \tag{32d}$$

$$Q_\theta = \Big(L_{36}C_{3m}r^{-\beta_m-1} + (L_{37}C_{4m} + L_{38}C_{5m} + L_{39}C_{6m})r^{\beta_m-1} + L_{40}C_{6m}r^{-\beta_m+1} + \frac{p_mr}{(\beta_m-4)}\Big)\cos(\beta_m\theta), \tag{32e}$$

where L_i's are constants and some of them are given in Appendix A. When $0 < \beta_m < 1$ and using C_{im}'s which are obtained from the previous, Eqs. (32) can be simplified as follows:

$$M_r = \Big(L_1C_{3m}r^{-\beta_m} + L_9C_{4m}r^{\beta_m} + \frac{L_{10}p_mr^2}{(\beta_m^2-4)(\beta_m^2-16)}\Big)\sin(\beta_m\theta), \tag{33a}$$

$$M_\theta = \Big(L_{11}C_{3m}r^{-\beta_m} + L_{19}C_{4m}r^{\beta_m} + \frac{L_{20}p_mr^2}{(\beta_m^2-4)(\beta_m^2-16)}\Big)\sin(\beta_m\theta), \tag{33b}$$

$$M_{r\theta} = \Big(L_{21}C_{3m}r^{-\beta_m} + L_{29}C_{4m}r^{\beta_m} + \frac{L_{30}p_mr^2}{(\beta_m^2-4)(\beta_m^2-16)}\Big)\cos(\beta_m\theta), \tag{33c}$$

$$Q_r = \Big((L_{12}C_{4m} + L_{13}C_{5m} + L_{14}C_{6m})r^{\beta_m-1} + \frac{p_mr}{(\beta_m-4)}\Big)\sin(\beta_m\theta), \tag{33d}$$

$$Q_\theta = \Big(L_{36}C_{3m}r^{-\beta_m-1} + (L_{37}C_{4m} + L_{38}C_{5m} + L_{39}C_{6m})r^{\beta_m-1} + L_{40}C_{6m}r^{-\beta_m+1} + \frac{p_mr}{(\beta_m-4)}\Big)\cos(\beta_m\theta). \tag{33e}$$

It is easy to show that for $0 < \beta_m < 1$, the moment and shear force resultants are singular in the vicinity of the vertex of the sector plate ($r \to 0$). It can be seen that the moment resultants ($M_r,\ M_\theta$ and $M_{r\theta}$) vary in the form of $r^{-\beta_m}$ at the vertex of the sector plate. Also, the force resultants (Q_r and Q_θ) vary in the form of r^{β_m-1} for $0 < \beta_m < 1$ in the near of $r = 0$. It was seen

before, for $\beta_m > 1$, the three coefficients vanish ($C_{2m} = C_{3m} = C_{6m} = 0$). By performing the procedure as previous case, the moment and shear force resultants for $\beta_m > 1$ in the near of vertex of sector plate are

$$M_r = \left((L_5C_{1m} + L_6C_{4m} + L_7C_{5m})r^{\beta_m-2} + L_9C_{4m}r^{\beta_m} + \frac{L_{10}p_mr^2}{(\beta_m^2-4)(\beta_m^2-16)}\right)\sin(\beta_m\theta), \tag{34a}$$

$$M_\theta = \left((L_{15}C_{1m} + L_{16}C_{4m} + L_{17}C_{5m})r^{\beta_m-2} + L_{19}C_{4m}r^{\beta_m} + \frac{L_{20}p_mr^2}{(\beta_m^2-4)(\beta_m^2-16)}\right)\sin(\beta_m\theta), \tag{34b}$$

$$M_{r\theta} = \left((L_{25}C_{1m} + L_{26}C_{4m} + L_{27}C_{5m})r^{\beta_m-2} + L_{29}C_{4m}r^{\beta_m} + \frac{L_{30}p_mr^2}{(\beta_m^2-4)(\beta_m^2-16)}\right)\cos(\beta_m\theta), \tag{34c}$$

$$Q_r = \left((L_{12}C_{4m} + L_{13}C_{5m})r^{\beta_m-1} + \frac{p_mr}{(\beta_m-4)}\right)\sin(\beta_m\theta), \tag{34d}$$

$$Q_\theta = \left((L_{37}C_{4m} + L_{38}C_{5m})r^{\beta_m-1} + \frac{p_mr}{(\beta_m-4)}\right)\cos(\beta_m\theta). \tag{34e}$$

Considering Eqs. (34), it can be easily shown that the moment resultants are singular in the interval $1 < \beta_m < 2$ at the vertex, but they are finite for $\beta_m > 2$ as r approaches zero. Since the shear force resultants vary in the form of r^{β_m-1}, they are not singular for $\beta_m > 1$.

Similarly, applying the same procedure for the solution of $\beta_m = 2, 4$, it is easy to show that the moment and shear force resultants are finite at the vertex of sector plate.

5. DQ analog

Since no studies have been found for FG sector plates, in order to verify our results, it is also attempted to solve our problem using differential quadrature method (DQM). To this end, the sector plate is discretized into some grid points n_r and n_θ in the r and θ directions, respectively. Based on the DQM rules, given in Appendix B, the governing equations (2) can be discretized in the following form:

$$\begin{aligned}
&A_{11}\left(\sum_{n=1}^{n_r}A_{in}^{(2)}u_{nj} + \frac{1}{r_i}\sum_{n=1}^{n_r}A_{in}^{(1)}u_{nj} - \frac{u_{ij}}{r_i^2} - \frac{1}{r_i^2}\sum_{n=1}^{n_\theta}A_{jn}^{(1)}v_{in} + \frac{1}{r_i}\sum_{n=1}^{n_r}\sum_{m=1}^{n_\theta}A_{in}^{(1)}A_{jm}^{(1)}v_{nm}\right)\\
&+A_{33}\left(\frac{1}{r_i^2}\sum_{n=1}^{n_\theta}A_{jn}^{(2)}u_{in} - \frac{1}{r_i}\sum_{n=1}^{n_r}\sum_{m=1}^{n_\theta}A_{in}^{(1)}A_{jm}^{(1)}v_{nm} - \frac{1}{r_i^2}\sum_{n=1}^{n_\theta}A_{jn}^{(1)}v_{in}\right)\\
&+B_{11}\left(\sum_{n=1}^{n_r}A_{in}^{(2)}\psi_{rnj} + \frac{1}{r_i}\sum_{n=1}^{n_r}A_{in}^{(1)}\psi_{rnj} - \frac{\psi_{r_{ij}}}{r_i^2} - \frac{1}{r_i^2}\sum_{n=1}^{n_\theta}A_{jn}^{(1)}\psi_{\theta n} + \frac{1}{r_i}\sum_{n=1}^{n_r}\sum_{m=1}^{n_\theta}A_{in}^{(1)}A_{jm}^{(1)}\psi_{\theta nm}\right)\\
&+B_{33}\left(\frac{1}{r_i^2}\sum_{n=1}^{n_\theta}A_{jn}^{(2)}\psi_{rin} - \frac{1}{r_i}\sum_{n=1}^{n_r}\sum_{m=1}^{n_\theta}A_{in}^{(1)}A_{jm}^{(1)}\psi_{\theta nm} - \frac{1}{r_i^2}\sum_{n=1}^{n_\theta}A_{jn}^{(1)\psi_{\theta in}}\right) = 0,
\end{aligned} \tag{35a}$$

$$\begin{aligned}
&A_{11}\left(\frac{1}{r_i}\sum_{n=1}^{n_r}\sum_{m=1}^{n_\theta}A_{in}^{(1)}A_{jm}^{(1)}u_{nm} + \frac{1}{r_i^2}\sum_{n=1}^{n_\theta}A_{jn}^{(1)}u_{in} + \frac{1}{r_i^2}\sum_{n=1}^{n_\theta}A_{jn}^{(2)}v_{in}\right)\\
&+A_{33}\left(\frac{1}{r_i^2}\sum_{n=1}^{n_\theta}A_{jn}^{(1)}u_{in} - \frac{1}{r_i}\sum_{n=1}^{n_r}\sum_{m=1}^{n_\theta}A_{in}^{(1)}A_{jm}^{(1)}u_{nm} + \sum_{n=1}^{n_r}A_{in}^{(2)}v_{nj} + \frac{1}{r_i}\sum_{n=1}^{n_r}A_{in}^{(1)}v_{nj} - \frac{v_{ij}}{r_i^2}\right)\\
&+B_{11}\left(\frac{1}{r_i}\sum_{n=1}^{n_r}\sum_{m=1}^{n_\theta}A_{in}^{(1)}A_{jm}^{(1)}\psi_{rnm} + \frac{1}{r_i^2}\sum_{n=1}^{n_\theta}A_{jn}^{(1)}\psi_{rin} + \frac{1}{r_i^2}\sum_{n=1}^{n_\theta}A_{jn}^{(2)}\psi_{\theta in}\right)\\
&+B_{33}\left(\frac{1}{r_i^2}\sum_{n=1}^{n_\theta}A_{jn}^{(1)}\psi_{rin} - \frac{1}{r_i}\sum_{n=1}^{n_r}\sum_{m=1}^{n_\theta}A_{in}^{(1)}A_{jm}^{(1)}\psi_{rnm} + \sum_{n=1}^{n_r}A_{in}^{(2)}\psi_{\theta nj} + \frac{1}{r_i}\sum_{n=1}^{n_r}A_{in}^{(1)}\psi_{\theta nj} - \frac{\psi_{\theta ij}}{r_i^2}\right) = 0,
\end{aligned} \tag{35b}$$

$$\begin{aligned}
&B_{11}\left(\sum_{n=1}^{n_r}A_{in}^{(2)}u_{nj} + \frac{1}{r_i}\sum_{n=1}^{n_r}A_{in}^{(1)}u_{nj} - \frac{u_{ij}}{r_i^2} - \frac{1}{r_i^2}\sum_{n=1}^{n_\theta}A_{jn}^{(1)}v_{in} + \frac{1}{r_i}\sum_{n=1}^{n_r}\sum_{m=1}^{n_\theta}A_{in}^{(1)}A_{jm}^{(1)}v_{nm}\right)\\
&+B_{33}\left(\frac{1}{r_i^2}\sum_{n=1}^{n_\theta}A_{jn}^{(2)}u_{in} - \frac{1}{r_i}\sum_{n=1}^{n_r}\sum_{m=1}^{n_\theta}A_{in}^{(1)}A_{jm}^{(1)}v_{nm} - \frac{1}{r_i^2}\sum_{n=1}^{n_\theta}A_{jn}^{(1)}v_{in}\right)\\
&+D_{11}\left(\sum_{n=1}^{n_r}A_{in}^{(2)}\psi_{rnj} + \frac{1}{r_i}\sum_{n=1}^{n_r}A_{in}^{(1)}\psi_{rnj} - \frac{\psi_{rij}}{r_i^2} - \frac{1}{r_i^2}\sum_{n=1}^{n_\theta}A_{jn}^{(1)}\psi_{\theta in} + \frac{1}{r_i}\sum_{n=1}^{n_r}\sum_{m=1}^{n_\theta}A_{in}^{(1)}A_{jm}^{(1)}\psi_{\theta nm}\right)\\
&+D_{33}\left(\frac{1}{r_i^2}\sum_{n=1}^{n_\theta}A_{jn}^{(2)}\psi_{rin} - \frac{1}{r_i}\sum_{n=1}^{n_r}\sum_{m=1}^{n_\theta}A_{in}^{(1)}A_{jm}^{(1)}\psi_{\theta nm} - \frac{1}{r_i^2}\sum_{n=1}^{n_\theta}A_{jn}^{(1)}\psi_{\theta in}\right) - K^2A_{33}\left(\psi_{rij} + \sum_{n=1}^{n_r}A_{in}^{(1)}w_{nj}\right) = 0,
\end{aligned} \tag{35c}$$

$$
\begin{aligned}
&B_{11}\left(\frac{1}{r_i}\sum_{n=1}^{n_r}\sum_{m=1}^{n_\theta}A_{in}^{(1)}A_{jm}^{(1)}u_{nm}+\frac{1}{r_i^2}\sum_{n=1}^{n_\theta}A_{jn}^{(1)}u_{in}+\frac{1}{r_i^2}\sum_{n=1}^{n_\theta}A_{jn}^{(2)}v_{in}\right)\\
&+B_{33}\left(\frac{1}{r_i^2}\sum_{n=1}^{n_\theta}A_{jn}^{(1)}u_{in}-\frac{1}{r_i}\sum_{n=1}^{n_r}\sum_{m=1}^{n_\theta}A_{in}^{(1)}A_{jm}^{(1)}u_{nm}+\sum_{n=1}^{n_r}A_{in}^{(2)}v_{nj}+\frac{1}{r_i}\sum_{n=1}^{n_r}A_{in}^{(1)}v_{nj}-\frac{v_{ij}}{r_i^2}\right)\\
&+D_{11}\left(\frac{1}{r_i}\sum_{n=1}^{n_r}\sum_{m=1}^{n_\theta}A_{in}^{(1)}A_{jm}^{(1)}\psi_{rnm}+\frac{1}{r_i^2}\sum_{n=1}^{n_\theta}A_{jn}^{(1)}\psi_{rin}+\frac{1}{r_i^2}\sum_{n=1}^{n_\theta}A_{jn}^{(2)}\psi_{\theta in}\right)\\
&+D_{33}\left(\frac{1}{r_i^2}\sum_{n=1}^{n_\theta}A_{jn}^{(1)}\psi_{rin}-\frac{1}{r_i}\sum_{n=1}^{n_r}\sum_{m=1}^{n_\theta}A_{in}^{(1)}A_{jm}^{(1)}\psi_{rnm}+\sum_{n=1}^{n_r}A_{in}^{(2)}\psi_{\theta nj}+\frac{1}{r_i}\sum_{n=1}^{n_r}A_{in}^{(1)}\psi_{\theta nj}-\frac{\psi_{\theta ij}}{r_i^2}\right)\\
&-K^2A_{33}\left(\psi_{\theta ij}+\frac{1}{r_i}\sum_{n=1}^{n_\theta}A_{jn}^{(1)}w_{in}\right)=0,
\end{aligned}
\tag{35d}
$$

$$
K^2A_{33}\left(\sum_{n=1}^{n_r}A_{in}^{(2)}w_{nj}+\frac{1}{r_i}\sum_{n=1}^{n_r}A_{in}^{(1)}w_{nj}+\frac{1}{r_i^2}\sum_{n=1}^{n_\theta}A_{jn}^{(2)}w_{in}+\sum_{n=1}^{n_r}A_{in}^{(1)}\psi_{rnj}+\frac{\psi_{rij}}{r_i}+\frac{1}{r_i}\sum_{n=1}^{n_\theta}A_{jn}^{(1)}\psi_{\theta in}\right)=-p_{ij}. \tag{35e}
$$

The boundary conditions can be also discretized at the circular and straight edges of the sector plate in a similar manner.

Eqs. (35) can be shown in the matrix form as

$$
[A_1]\{F_B\}+[A_2]\{F_I\}=\{P\}, \tag{36}
$$

where $\{F_B\}$ and $\{F_I\}$ are the boundary and domain degrees of freedom vectors, respectively, these vectors can be written as:

$$
\{F_I\}=\begin{Bmatrix}\{u_I\}\\ \{v_I\}\\ \{w_I\}\\ \{\psi_{rI}\}\\ \{\psi_{\theta I}\}\end{Bmatrix},\quad \{F_B\}=\begin{Bmatrix}\{u_B\}\\ \{v_B\}\\ \{w_B\}\\ \{\psi_{rB}\}\\ \{\psi_{\theta B}\}\end{Bmatrix}, \tag{37}
$$

where

$$
\begin{aligned}
&\{u_I\}=\begin{bmatrix}u_{22} & u_{23} & \dots & u_{(N_r-1)(N_\theta-1)}\end{bmatrix},\quad \{u_B\}=\begin{bmatrix}u_{11} & u_{12} & \dots & u_{N_rN_\theta}\end{bmatrix},\\
&\{v_I\}=\begin{bmatrix}v_{22} & v_{23} & \dots & v_{(N_r-1)(N_\theta-1)}\end{bmatrix},\quad \{v_B\}=\begin{bmatrix}v_{11} & v_{12} & \dots & v_{N_rN_\theta}\end{bmatrix},\\
&\{w_I\}=\begin{bmatrix}w_{22} & w_{23} & \dots & w_{(N_r-1)(N_\theta-1)}\end{bmatrix},\quad \{w_B\}=\begin{bmatrix}w_{11} & w_{12} & \dots & w_{N_rN_\theta}\end{bmatrix},\\
&\{\psi_{rI}\}=\begin{bmatrix}\psi_{r22} & \psi_{r23} & \dots & \psi_{r(N_r-1)(N_\theta-1)}\end{bmatrix},\quad \{\psi_{rB}\}=\begin{bmatrix}\psi_{r11} & \psi_{r12} & \dots & \psi_{rN_rN_\theta}\end{bmatrix},\\
&\{\psi_{\theta I}\}=\begin{bmatrix}\psi_{\theta 22} & \psi_{\theta 23} & \dots & \psi_{\theta(N_r-1)(N_\theta-1)}\end{bmatrix},\quad \{\psi_{\theta B}\}=\begin{bmatrix}\psi_{\theta 11} & \psi_{\theta 12} & \dots & \psi_{\theta N_rN_\theta}\end{bmatrix}.
\end{aligned}
\tag{38}
$$

Also the discretized boundary conditions can be formed as the following matrix equation as

$$
[A_3]\{F_B\}+[A_4]\{F_I\}=0. \tag{39}
$$

Obtaining the boundary degrees of freedom vector from Eq. (39) and substituting the result into Eq. (36), yields

$$
\{F_I\}=([A_2]-[A_1][A_3]^{-1}[A_4])^{-1}\{P\}. \tag{40}
$$

It is clear that the plate responses can be obtained by solving Eq. (40). It is noticeable that to obtain the results for sector plate in DQM, the annular sector plate with inner to outer radius of 10^{-7} ($r_i/a=10^{-7}$) is solved.

6. Numerical results

To present the numerical results, SUS304 and Si3N4 are used as the metal and ceramic in FG plate, respectively. The Poisson's ratio of 0.3 has been used. The quantity of the applied uniform load is supposed to be $P_0=1$ and the shear correction factor is assumed to be $K^2=5/6$. Also, $T=300$ K is used as the temperature value.

Also, for numerical results in figures, the geometric properties of the sector plate such as thickness-radius ratio, and sector angle are assumed to be 0.2 and $\frac{\pi}{3}$, respectively (the unit of the length is meter).

In order to verify the accuracy of the present results, the deflection of the FG sector plate is also obtained using differential quadrature method (DQM). The convergent study of maximum deflection of a FG plate with two simply supported radial

edges and free circular edge is shown in Table 2 for various powers of the functionally graded material. The sector angle is 60° and the number of node in θ direction is considered $n_\theta = 25$ and the number of node in r direction (n_r) varies from 13 to 20 nodes. The results indicate the convergence of the solution.

Tables 3–5 show the transverse deflection of a sector plate with clamped, simply supported and free circular edge, respectively, which is obtained from the mentioned exact method in comparison with the DQM results. The non-dimensional transverse displacement $\left(\bar{w} = \frac{A_{11}}{P_0 h^2} w\right)$ is considered at the middle line of the sector plate $(\theta = \alpha/2)$ and $r = 0.25, 0.5$ and 0.75. From these tables, it can be found that the present formulations are accurate.

Table 2
The convergence of the maximum transverse displacement of the sector plate on the free edge ($\alpha = 60^\circ,\ h/a = 0.2,\ n_\theta = 25$).

n	n_r								Exact
	13	14	15	16	17	18	19	20	
0	102.0422	102.0447	102.0454	102.0456	102.0457	102.0457	102.0457	102.0457	102.0458
0.5	104.3205	104.3232	104.3240	104.3242	104.3243	104.3243	104.3243	104.3243	104.3243
1	103.5050	103.5077	103.5085	103.5087	103.5087	103.5087	103.5087	103.5087	103.5088
2	100.8557	100.8580	100.8587	100.8589	100.8589	100.8589	100.8589	100.8589	100.8590

Table 3
A comparison study of the transverse displacement for a FG sector plate with clamped circular edge.

α	n	Method	$h/a = 0.1$			$h/a = 0.2$		
			0.25	0.5	0.75	0.25	0.5	0.75
30	1	Exact	1.6586	11.7274	20.4431	0.2586	1.3549	2.2940
		DQM	1.6586	11.7274	20.4431	0.2586	1.3255	2.2940
	2	Exact	1.6352	11.4872	20.0273	0.2572	1.3102	2.2665
		DQM	1.6352	11.4872	20.0272	0.2572	1.3102	2.2665
60	1	Exact	23.6755	80.7456	71.3552	2.2593	7.2164	7.0044
		DQM	23.6755	80.7455	71.3550	2.2593	7.2164	7.0044
	2	Exact	23.1271	78.8054	69.7427	2.2247	7.0932	6.8998
		DQM	23.1271	78.8053	69.7425	2.2247	7.0931	6.8998

Table 4
A comparison study of the transverse displacement for a FG sector plate with simply supported circular edge.

α	n	Method	$h/a = 0.1$			$h/a = 0.2$		
			0.25	0.5	0.75	0.25	0.5	0.75
30	1	Exact	1.6728	12.4518	25.2544	0.2593	1.3599	2.5226
		DQM	1.6728	12.4518	25.2544	0.2593	1.3599	2.5226
	2	Exact	1.6489	12.1885	24.6851	0.2578	1.3434	2.4870
		DQM	1.6489	12.1885	24.6850	0.2578	1.3434	2.4870
60	1	Exact	27.8932	107.7284	124.2744	2.4924	8.7077	9.9316
		DQM	27.8934	107.7285	124.2741	2.4924	8.7077	9.9315
	2	Exact	27.2202	104.9914	121.0999	2.4503	8.5367	9.7332
		DQM	27.2204	104.9914	121.0997	2.4503	8.5366	9.7331

Table 5
A comparison study of the transverse displacement for a FG sector plate with free circular edge.

α	n	Method	$h/a = 0.1$				$h/a = 0.2$			
			0.25	0.5	0.75	1	0.25	0.5	0.75	1
30	1	Exact	1.7179	15.1295	51.7162	116.1560	0.2625	1.5528	4.4959	9.2223
		DQM	1.7179	15.1296	51.7162	116.1559	0.2625	1.5528	4.4959	9.2223
	2	Exact	1.6929	14.7946	50.4510	113.2058	0.2609	1.5319	4.4166	9.0327
		DQM	1.6929	14.7946	50.4510	113.2057	0.2609	1.5319	4.4166	9.0327
60	1	Exact	57.7407	337.2656	84.2907	1533.2566	4.4521	23.8551	58.0112	103.5088
		DQM	57.7412	337.2663	846.2911	1533.2562	4.4522	23.8551	58.0112	103.5087
	2	Exact	56.2421	328.1938	823.2758	1491.4075	4.3583	23.2864	56.5633	100.8590
		DQM	56.2425	328.1945	823.2762	1491.4072	4.3584	23.2864	56.5633	100.8589

In order to study the effects of boundary layer function, this function is depicted for different powers of FGM in Figs. 2 and 3 for the FG sector plate with clamped and free circular edge, respectively. It should be noticed that $\overline{\Phi}$ is the boundary layer function multiply by $10^{12}(\overline{\Phi} = \varphi_4 * 10^{12})$. It can be seen that this function has significant effect on the edges of the plate

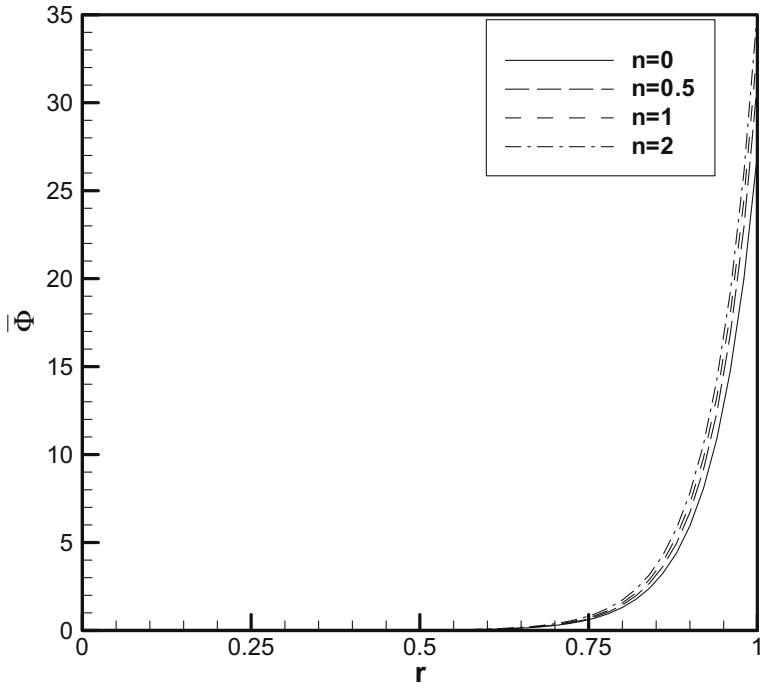

Fig. 2. The variation of the boundary layer function along the radial direction of FG sector plate with clamped circular edge.

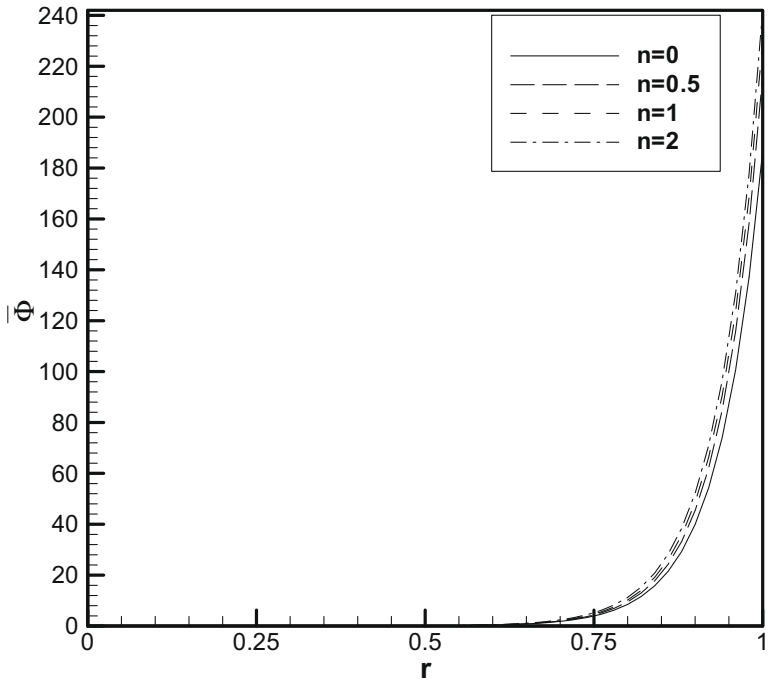

Fig. 3. The variation of the boundary layer function along the radial direction of FG sector plate with free circular edge.

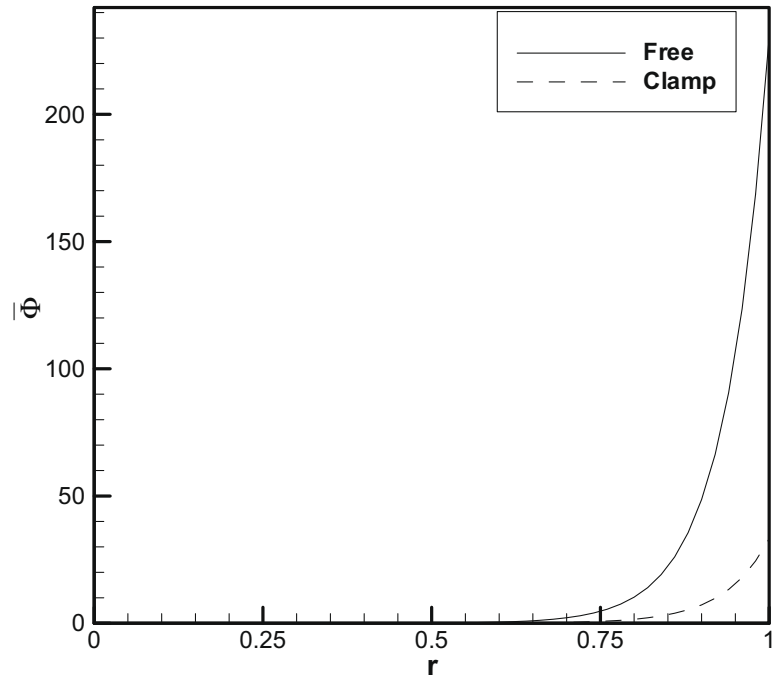

Fig. 4. A comparison of the boundary layer function of clamped and free sector plate ($n = 1$).

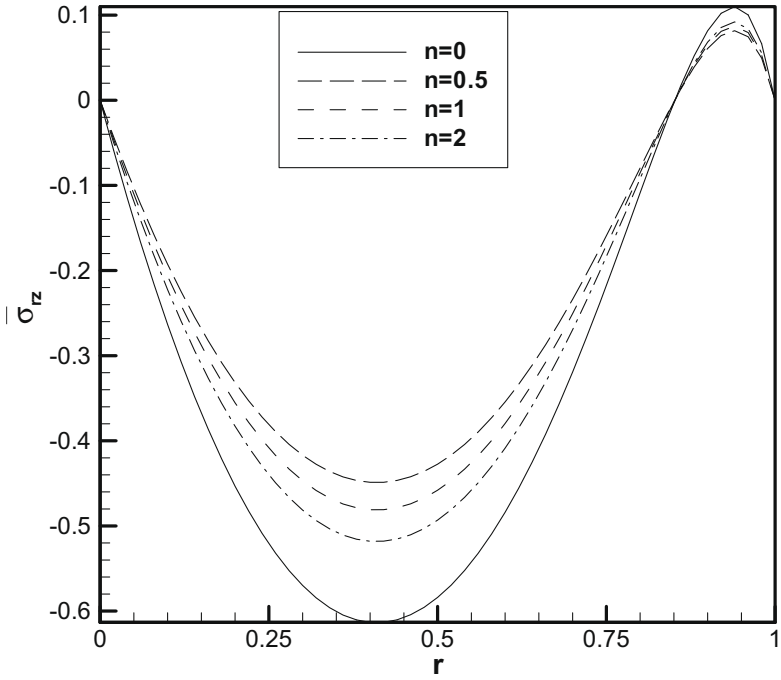

Fig. 5. Non-dimensional shear stress of the FG sector plate vs. radius.

hence it can be called the boundary layer function. Also, it can be concluded that with increasing the power of FGM, the width of this function increases. The boundary layer functions of clamped and free sector plate are shown in Fig. 4. It can be found that the effect of this function on free edge is more than that of clamped edge.

The variation of the out of plane shear stress σ_{rz} has been depicted across the radial edges in Fig. 5 for various powers of FGM. The FG sector plate has free boundary condition at the circular edge.

7. Conclusion

In the present work, the singularity and boundary layer effect in the functionally graded sector plate have been studied. The governing equilibrium equations of FG sector plate have been obtained based on the first-order shear deformation plate theory. These highly coupled partial differential equations have been decoupled and solved using an analytical method. It is seen that there are singularities for moments and shear forces at the vertex of the FG sector plate. Also, it has been shown that the effects of boundary layer function of the FG plate are similar to isotropic one. Since the effect of boundary layer function for FG plate is similar to isotropic and composite plates, this function seems to be material independent. Finally, in order to verify the accuracy of the result, the governing equations of FG sector plate have been also solved using differential quadrature method.

Appendix A

The coefficients of the moment resultant are given as follows:

$$L_1 = -\left(-\frac{B_{11}^2\beta_m^2}{A_{11}} + 2D_{12} - D_{12}\beta_m - D_{12}\beta_m^2 + 2D_{11} + \frac{3B_{11}^2\beta_m}{A_{11}} - \frac{2B_{11}^2}{A_{11}} - \frac{2B_{12}B_{11}}{A_{11}}\,\frac{B_{12}B_{11}\beta_m^2}{A_{11}} + \frac{B_{12}B_{11}\beta_m}{A_{11}} - 3D_{11}\beta_m + D_{11}\beta_m^2\right), \tag{A.1}$$

$$L_2 = \beta_m\left(\frac{B_{11}^2}{A_{11}} - D_{11}\beta_m + D_{12}\beta_m + D_{12} - D_{11} + \frac{B_{11}^2\beta_m}{A_{11}} + \frac{B_{11}^2}{A_{11}} - \frac{B_{12}B_{11}\beta_m}{A_{11}}\right), \tag{A.2}$$

$$\begin{aligned} L_3 = {} & -(-\widehat{D}B_{11}^2\beta_m^3 - 4\widehat{D}B_{11}^2\beta_m - 4\widehat{D}B_{12}B_{11}\beta_m^3 + 4\widehat{D}B_{12}B_{11}\beta_m - 4D_{11}\widehat{D}A_{11}\beta_m^3 + 4D_{11}\widehat{D}A_{11}\beta_m - 4D_{12}\widehat{D}A_{11}\beta_m \\ & + 4D_{12}\widehat{D}A_{11}\beta_m^3)/(A_{11}K^2\widehat{A}), \end{aligned} \tag{A.3}$$

$$L_4 = -\frac{1}{2}\frac{2^{\beta_m}\mu^{-\beta_m}\widehat{C}\,\Gamma(\beta_m)^2\beta_m(\beta_m+1)(-B_{12}B_{11} + B_{11}^2 - D_{11}A_{11} + D_{12}A_{11})}{A_{11}K^2\widehat{A}\,\Gamma(\beta_m-1)(\beta_m-1)}, \tag{A.4}$$

$$L_5 = \beta_m\left(-\frac{B_{11}^2}{A_{11}} - D_{11}\beta_m + D_{12}\beta_m - D_{12} + D_{11} + \frac{B_{11}^2\beta_m}{A_{11}} - \frac{B_{12}B_{11}\beta_m}{A_{11}} + \frac{B_{12}B_{11}}{A_{11}}\right), \tag{A.5}$$

$$\begin{aligned} L_6 = {} & (4\widehat{D}B_{11}^2\beta_m^3 - 4\widehat{D}B_{11}^2\beta_m - 4\widehat{D}B_{12}B_{11}\beta_m^3 + 4\widehat{D}B_{12}B_{11}\beta_m - 4D_{11}\widehat{D}A_{11}\beta_m^3 + 4D_{11}\widehat{D}A_{11}\beta_m - 4D_{12}\widehat{D}A_{11}\beta_m \\ & + 4D_{12}\widehat{D}A_{11}\beta_m^3)/(A_{11}K^2\widehat{A}), \end{aligned} \tag{A.6}$$

$$L_7 = \frac{\widehat{C}\,2^{-\beta_m}\mu^{\beta_m}(-B_{12}B_{11} + B_{11}^2 - D_{11}A_{11} + D_{12}A_{11})}{A_{11}K^2\widehat{A}\,\Gamma(\beta_m-1)}, \tag{A.7}$$

$$L_8 = -\frac{1}{2}\frac{2^{-\beta_m}\mu^{\beta_m}\widehat{C}\,\pi(\beta_m-1)(-B_{12}B_{11} + B_{11}^2 - D_{11}A_{11} + D_{12}A_{11})}{A_{11}K^2\widehat{A}\,\Gamma(\beta_m-1)(\beta_m-1)}, \tag{A.8}$$

$$L_9 = \frac{2B_{11}^2}{A_{11}} - D_{11}\beta_m^2 + \frac{2B_{12}B_{11}}{A_{11}} + \frac{B_{12}B_{11}\beta_m}{A_{11}} - \frac{B_{12}B_{11}\beta_m^2}{A_{11}} - 3D_{11}\beta_m + D_{12}\beta_m^2 + \frac{3B_{11}^2\beta_m}{A_{11}} - 2D_{11} - 2D_{12} + \frac{B_{11}^2\beta_m^2}{A_{11}} - D_{12}\beta_m, \tag{A.9}$$

$$L_{10} = -\frac{4B_{12}B_{11}}{\widehat{D}A_{11}} - \frac{12B_{11}^2}{\widehat{D}A_{11}} + \frac{B_{12}B_{11}\beta_m^2}{\widehat{D}A_{11}} + \frac{12D_{11}}{\widehat{D}} - \frac{D_{12}\beta_m^2}{\widehat{D}} + \frac{4D_{12}}{\widehat{D}}. \tag{A.10}$$

Appendix B

According to the DQ method rules, the partial derivative of a function with respect to a space variable is approximated by a weighted linear combination of the function values at the grid points. The mth derivative of the function $f(r,\theta)$ with respect to r and θ, respectively, can be written as

$$\begin{aligned} \frac{\partial^m f(r_i,\theta_j)}{\partial r^m} &= \sum_{n=1}^{n_r} A_{in}^{(m)} f(r_n,\theta_j) \\ \frac{\partial^m f(r_i,\theta_j)}{\partial \theta^m} &= \sum_{n=1}^{n_\theta} A_{jn}^{(m)} f(r_i,\theta_n) \quad \text{for } i = 1,\ldots,n_r,\ j = 1,\ldots,n_\theta, \end{aligned} \tag{B.1}$$

where $A_{pq}^{(m)}$ are the weighting coefficients related to the mth order derivative. The off-diagonal and diagonal weighting elements related to the first-order derivative are defined as follows, respectively:

$$\begin{aligned} A_{pq}^{(1)} &= \frac{M(x_p)}{(x_p - x_q)M(x_q)} \quad \text{for } p \neq q,\ p,q = 1,2,\ldots,\ n_x, \\ A_{pp}^{(1)} &= -\sum_{\substack{q=1 \\ q\neq p}}^{n_x} A_{pq}^{(1)}, \end{aligned} \tag{B.2}$$

where x is the independent variable (r,θ) and the partial derivative is defined with respect to it. $M(x_i)$ is given as:

$$M(x_p) = \prod_{\substack{q=1 \\ q\neq p}}^{n_x} (x_p - x_q). \tag{B.3}$$

The following relationship is given for evaluating the weighting coefficients of higher-order derivatives:

$$\begin{aligned} A_{pq}^{(m)} &= m\left[A_{pp}^{(m-1)}A_{pq}^{(1)} - \frac{A_{pq}^{(m-1)}}{x_p - x_q}\right] \quad \text{for } p \neq q,\ p,q = 1,2,\ldots,n_x, \\ A_{pp}^{(m)} &= -\sum_{\substack{q=1 \\ q\neq p}}^{n_x} A_{pq}^{(m)}. \end{aligned} \tag{B.4}$$

In the present study the Gauss–Chebyshev–Lobatto is used to locate the grid points,

$$\begin{aligned} r_i &= \frac{a}{2}\left(1 - \cos\left(\frac{(i-1)\pi}{n_r - 1}\right)\right) \quad \text{for } i = 1,2,\ldots,n_r, \\ \theta_j &= \frac{\theta}{2}\left(1 - \cos\left(\frac{(j-1)\pi}{n_\theta - 1}\right)\right) \quad \text{for } j = 1,2,\ldots,n_\theta. \end{aligned} \tag{B.5}$$

References

[1] M.L. William, Stress singularities resulting from various boundary conditions in angular corners of plates under bending, in: Proceedings of 1st US National Congress of Applied Mechanics, 1952, pp. 325–329.
[2] M.L. William, Stress singularities resulting from various boundary conditions in angular corners of plates in extension, J. Appl. Mech. 19 (1952) 526–528.
[3] J.P. Dempsey, G.B. Sinclair, On the stress singularities in the plate elasticity of the composite wedge, J. Elast. 9 (1979) 373–391.
[4] I.O. Ojikutu, R.O. Low, R.A. Scott, Stress singularities in laminated composite wedge, Int. J. Solids Struct. 20 (1984) 777–790.
[5] A.W. Leissa, O.G. McGee, C.S. Huang, Vibrations of sectorial plates having corner stress singularities, ASME J. Appl. Mech. 60 (1993) 134–140.
[6] A.W. Leissa, O.G. McGee, C.S. Huang, Vibrations of circular plates having V-notches or sharp radial cracks, J. Sound Vib. 161 (1993) 227–239.
[7] C.S. Huang, A.W. Leissa, O.G. McGee, Exact analytical solutions for the vibrations of sectorial plates with simply supported radial edges, ASME J. Appl. Mech. 60 (1993) 478–483.
[8] W.S. Burton, G.B. Sinclair, On the singularities in Reissner's theory for the bending of elastic plates, ASME J. Appl. Mech. 53 (1986) 220–222.
[9] C.S. Huang, O.G. McGee, A.W. Leissa, Exact analytical solutions for the vibrations of Mindlin sectorial plates with simply supported radial edges, Int. J. Solids Struct. 31 (1994) 1609–1631.
[10] C.S. Huang, Stress singularities at angular corners in first-order shear deformation plate theory, Int. J. Mech. Sci. 45 (2003) 1–20.
[11] A. Kotousov, Y.T. Lew, Stress singularities resulting from various boundary conditions in angular corners of plates of arbitrary thickness in extension, Int. J. Solids Struct. 43 (2006) 5100–5109.
[12] R.J. Hartranft, G.C. Sih, The use of eigenfunction expansions in the general solution of three-dimensional crack problems, J. Math. Mech. 19 (1969) 123–138.
[13] M. Xie, R.A. Chaudhuri, Three-dimensional stress singularity at a bimaterial interface crack front, Compos. Struct. 40 (1998) 137–147.
[14] C.S. Huang, Corner stress singularities in a high-order plate theory, Comput. Struct. 82 (2004) 1657–1669.
[15] A.M. Zenkour, Generalized shear deformation theory for bending analysis of functionally graded plates, Appl. Math. Model. 30 (2006) 67–84.
[16] C.S. Huang, M.J. Chang, Corner stress singularities in an FGM thin plate, Int. J. Solids Struct. 44 (2007) 2802–2819.
[17] E. Reissner, The effect of transverse shear deformation on the bending of elastic plates, J. Appl. Mech. 12 (1945) 69–77.
[18] E. Reissner, Reflections on the theory of elastic plates, Appl. Mech. Rev. 38 (1985) 1453–1464.
[19] A. Nosier, J.N. Reddy, On boundary layer and interior equations for higher-order theories of plates, ZAMM 72 (1992) 657–666.
[20] A. Nosier, A. Yavari, S. Sarkani, A study of the edge-zone equation of Mindlin–Reissner plate theory in bending of laminated rectangular plates, Acta Mech. 146 (2001) 227–238.
[21] E. Jomehzadeh, A.R. Saidi, Analytical solution for free vibration of transversely isotropic sector plates using a boundary layer function, Thin-Walled Struct. 47 (2009) 82–88.
[22] E. Jomehzadeh, A.R. Saidi, S.R. Atashipour, An analytical approach for stress analysis of functionally graded annular sector plates, Mater. Des. 30 (2009) 3679–3685.
[23] S.R. Atashipour, A.R. Saidi, E. Jomehzadeh, On the boundary layer phenomenon in bending of thick annular sector plates using third-order shear deformation theory, Acta. Mech. 211 (2010) 89–99.
[24] Y.S. Touloukian, Thermophysical Properties of High Temperature Solid Materials, MacMillan, New York, 1967.
[25] J. Yang, H.S. Shen, Vibration characteristics and transient response of shear-deformable functionally graded plates in thermal environments, J. Sound Vib. 255 (2002) 579–602.